

LONG-TERM DAMAGE OF HISTORIC MASONRY: A PROBABILISTIC MODEL

Anna Anzani

Politecnico di Milano, Department of Structural Engineering, Milano, ITALY
anzani@stru.polimi.it

Elsa Garavaglia

Politecnico di Milano, Department of Structural Engineering, Milano, ITALY
garava@stru.polimi.it

Luigia Binda

Politecnico di Milano, Department of Structural Engineering, Milano, ITALY
binda@stru.polimi.it

Abstract: Creep and the creep-fatigue interaction have shown to strongly influence the mechanical behaviour of ancient masonry and long-term heavy loads proved to cause a continuous damage. The problem of achieving a reliable lifetime estimate of historic masonry toward the effects of persistent loading has been dealt with by a probabilistic approach. The results of pseudo-creep tests on ancient masonry of different ages and their interpretation through a probabilistic model are presented, aimed to the individuation of a random variable as a significant index of vulnerability, and to the solution of the classic problem of reliability in stochastic conditions.

NOTATION

r.v.	random variable
σ	vertical peak stress
σ_v	vertical stress
σ_v^*	constant vertical stress level
ε_v^{\max}	maximum vertical strain
ε_h^{\max}	maximum horizontal strain
$\dot{\varepsilon}_v, \dot{\varepsilon}_h$	vertical and horizontal strain-rate
$\bar{\dot{\varepsilon}}_h, \bar{\dot{\varepsilon}}_v$	critical strain-rate levels
$\bar{\sigma}$	vertical stress value required to exceed $\bar{\dot{\varepsilon}}_v$ or $\bar{\dot{\varepsilon}}_h$

p.d.f.	probability density function
c.d.f.	cumulative distribution function
\dot{E}	critical value of $\dot{\varepsilon}$
$f_{\dot{\varepsilon}}(\dot{E})$	p.d.f. of critical $\dot{\varepsilon}_v$ or $\dot{\varepsilon}_h$
$F_{\dot{\varepsilon}}(\dot{E})$	c.d.f. of the above p.d.f.
$\phi_{\dot{\varepsilon}}(\dot{E})$	failure rate function of the above p.d.f.
$\mathfrak{S}_{\dot{\varepsilon}}(\dot{E})$	survive function of the above p.d.f.
α_1, ρ_1	parameters of Weibull density (eq.2)
t	time
$R(t)$	reliability function
$\bar{R}(\sigma_v)$	probability not to exceed the strain-rate level $\bar{\dot{\varepsilon}}$
$F_{\bar{\sigma}}(\sigma_v)$	c.d.f. of $\bar{\sigma}$
$f_{\bar{\sigma}}(\sigma_v)$	p.d.f. of the above p.d.f.
$\phi_{\bar{\sigma}}(\sigma_v)$	failure rate function of the above p.d.f.
exp	$e = 2.718281828$
$F_{\bar{\sigma}^*}(\sigma_v)$	experimental fragility curve
b_1, b_2, α and ρ	shape parameters
u	variable

INTRODUCTION

The main part of the European territory is characterized by the presence of historic masonry structures often characterized by non-homogeneous load-bearing sections that, during their service life, can be subjected to decay due to aggressive environmental attacks, aging and damage due to

long term heavy loads. Together with other synergetic aspects, time dependent behaviour has proved to be involved in the collapse of historical buildings occurred during the last twenty years including the recent failures of the Meldert Bell-tower and the Maagdentoren Tower at Zichem (Belgium, 2006). The conservation of the pre-existing heritage gains an increasing relevance toward the safeguard of the memory and the complex relationship that the architectural culture has to carry out with its past, in view of a responsible and sustainable future. Among the risk factors menacing the safety of ancient structures, in addition to external factors like the lack of maintenance, the load increase due to building modifications, soil settlements, mechanical shocks due to earthquakes, fires, etc., an intrinsic feature of masonry (as of any rock-like materials) has to be highlighted. This feature, basically related to the self-weight and denominated time-dependent behaviour or creep, had not been recognized as a structurally crucial aspect, probably because it develops in the long run. Although it was well known in mining engineering and rock and soil mechanics [1], it had never been considered a risk factor in the safety assessment of ancient masonry buildings. The influence of time becomes evident for instance in compressive tests at vertical constant load. In particular, if a vertical constant load is applied to a masonry specimen, an increase in the vertical and horizontal deformation takes place, which is commonly subdivided into three phases (Fig. 1): the so-called primary, secondary and tertiary creep [2], respectively corresponding to the visco-elastic branch at decreasing strain rate (decreasing slope of the diagram) and reversible strain; to the visco-plastic branch at a constant slope; to the final highly unstable branch, characterized by strain developing at increasing rate and ending with the specimen failure. The appearance of one or more of these phases and the strain rate of the secondary creep phase depends on the level of the applied constant stress. In view of the safeguard of historical buildings and of preventing their failure, the possibility of detecting secondary creep strain rate is mostly relevant. In fact, primary creep phase corresponds to a stable and safe behaviour and does not require any special care; on the contrary if the structures are already displaying tertiary creep, which is preliminary to failure, there may be any possibility left to carry out strengthening interventions in useful time. Therefore, detecting

secondary creep strain rate may give information on the residual service life, as commented below (see Fig. 10 for example). Though the estimate cannot have an absolute value, it is certainly valid on a comparative basis; in fact, it may allow public institutions to classify buildings according to their risk level and to define a priority for the required intervention campaigns.

As well known, these aspects of the problem suffer of uncertainty and may be dealt with through probabilistic approaches and or fuzzy sets theory.

The literature offers a good panorama of structural safety assessment approached throughout Monte Carlo simulation, genetic algorithms, fuzzy theory and so on [3], [4], [5], [6], [7], [8], [9], but the proposed approaches are prevalently applied on RC structures or steel structures simulating deterioration processes and only seldom the modelling is based on experimental data obtained by monitoring action of real structures. The reasons for that are: monitoring is expensive and requires long time of observation; modelling of the concrete deterioration process has reached a good level of definition [10].

Similar approaches are not applied to ancient masonry, since a lot of parameters are involved in its definition such that, at the moment, simulating its behaviour in a general form seems impossible.

All the efforts are addressed to model the mechanical behaviour of masonry [11], [12], [13], [14], [15], [16] but the results seem to be affected by uncertainty.

Since 1989 the authors are involved in a research program in which some experimental tests to investigate the masonry behaviour over time has been successfully developed [17], [18], [19].

Exploiting the medieval and the XVI century masonry coming from the ruins of the collapsed tower of Pavia and that coming from the XVI century crypt of the Cathedral of Monza, several experimental procedures have been adopted to understand the phenomenon, from creep to pseudo-creep tests at different time intervals, and various rheological models have been applied to describe the creep evolution and creep-induced damage [20].

The results obtained have put in evidence the necessity to consider a few uncertainties involved in the collapse of massive buildings, therefore a probabilistic approach has been proposed.

In the literature some examples are presented dealing with ancient masonry from a probabilistic point of view [21]. The choice of a probabilistic approach, in general not simple, is particularly complex in the case of masonry given the numerous uncertainties affecting it. In fact, a probabilistic approach depending on a lot of random variables (r.v.) is difficult to govern and, often, becomes unreliable. Therefore, the choice of a significant parameter able to consistently describe the time dependent deterioration process is a prior matter. The suitable choice of the r.v. describing the deterioration process can lead to model the process in a simple, but reliable, way.

By experimental evidence, the strain evolution connected with a given stress history of a viscous material like a historic masonry can be described through vertical and horizontal strain rate connected with a well defined creep phase.

Since the strain-rate is related to the residual life of the material, to model its evolution over stresses the *fragility curves approach* is proposed, greatly used in seismic vulnerability analysis. The method is simple and, if suitable data coming from monitoring of ancient buildings were available, it could be adopted for the safety evaluation of existing structures.

Aim of the paper is to suggest an experimental procedure suitable to study in the laboratory creep behaviour, and in particular to catch critical secondary creep strain rate and to propose a probabilistic approach for the estimate of the residual life of the material. Further development will be the application of the approach to the interpretation of data coming from long term monitoring of historic buildings in view of their safeguard and failure prevention.

EXPERIMENTAL ACTIVITY

Previous research

After the collapse of the Civic Tower of Pavia (XI to XVI century), during the investigation for searching the causes of the collapse, many prisms of different dimensions were obtained from the large blocks coming from the ruins of the tower [22] and constituting the medieval trunk of the structure (Figure 1). The prisms, subjected to mechanical tests, had mainly been obtained from the

conglomerate forming the very thick internal part of the 2800 mm three-leaf walls (Figure 2); a few of them were coming from the fairly regular external leaves made of brick masonry of thickness varying between 150 and 490 mm; no specimens were sampled from the plain masonry constituting the XVI century belfry, not involved in the initiation of the collapse. [22], [17], [18]. Purpose of the testing activity has been initially the identification of the creep behaviour as a possible cause of the collapse of buildings, once understood that the portion of tower where the failure started was the base (highest value of the vertical stress and its concentration due to the presence of a door and the staircase), then the study of factors affecting creep (rate of loading, stress level,...) and the set up of the most suitable testing procedures to understand the phenomenon, finally the individuation of significant parameters (strain rate of secondary creep phase, ...) that may be referred to as risk indicators in real structures. The prisms dimensions were initially 400x600x700 mm, i.e. the maximum compatible with the testing machine; subsequently they were progressively reduced to better exploit the available historic masonry, ending with prisms of 200x200x510 mm.

In addition to monotonic and cyclic tests (Figure 3), six prisms of dimensions 300×300×510 mm were tested in compression in controlled conditions of 20°C and 50% RH, using hydraulic machines able to keep constant a maximum load of 1000 kN. The load was applied in subsequent steps, kept constant until either the creep strain reached a constant value or a steady state was attained. The first stress level was chosen between 40% and 50% of the static peak stress of the prisms, estimated by sonic tests [17]. The strain vs. time diagrams of the prisms tested are reported in Figures 4a, b. From the experimental data, the development of all the creep phases was evident, with secondary creep showing even at 41% of the estimated material peak stress and tertiary creep showing at about 70%; material dilation took place under severe compressive stress corresponding to high values of the horizontal strain due to slow crack propagation until failure [17].

Considering that long term tests require constant thermo-hygrometric conditions and especially designed testing apparatus, a more rapid and therefore more convenient testing procedure was subsequently preferred. The so called pseudo-creep tests were carried out applying the load by

subsequent steps corresponding to a constant value (generally 0.25 or 0.3 MPa) kept constant for a specific time interval. Different durations of the time interval have been experimented from 300 to 28800 seconds that allowed to indirectly observe the influence of the rate of loading. In fact, these tests characterized by a regular load history tend to simulate, by discrete load steps, monotonic tests where the load increases continuously at an equivalent constant rate and give the opportunity to satisfactorily catch the limit between primary and secondary creep phase [17]. As an example, table 1 shows the results obtained on twelve prisms of dimensions 100 x 100 x 180 mm tested in compression by subsequent load steps corresponding to 0.3 MPa kept constant for different time intervals respectively of 300 sec, 900 sec, 3600 sec and 10800 sec. An initial step of 0.6 MPa was first applied. Before the application of any new load step, the sample was completely unloaded so the unloading Young modulus could be evaluated [23] (Figure 5). Looking at Table 1, it is interesting to notice that the average peak stress tends to decrease and the corresponding strain tends to increase at extending the time interval, indicating that the stress-strain behaviour is strongly time-dependent. The results of a test carried out at 10800 sec. are reported in Figure 5: at each load step primary creep occurred and, during the last load step, also secondary and tertiary creep took place.

Subsequently, the XVI century plain masonry (Figure 2) never tested before, because not responsible of the collapse trigger, was also studied. In fact, its behaviour may provide a useful comparison for other structures of the same age and constructive technique, being a historical masonry not usually available for mechanical testing.

Pseudo-creep tests

Before carrying out pseudo-creep tests, the material was characterized by monotonic tests and non-destructive sonic tests (Figure 6). In Figure 6b the compressive peak stress have been plotted vs. the sonic velocity comparing the results obtained on the tower of Pavia with those previously obtained on the crypt of Monza [26]. A direct relationship can be clearly observed; the prisms

obtained from the outer leaf of the medieval part of the tower of Pavia achieved the highest strength values, whereas the inner leaf the lowest ones, being the masonry of the belfry in between. In fact, this is coherent with the texture characteristics of the three materials (Figures 7 a-d). The outer leaf is the highest quality one, built to be the visible part of the structure; apparently its regular texture is in some way similar to that of the belfry, but probably the intrinsic characteristics of its mortar are higher; the inner leaf is constituted by rubble masonry. The values of the crypt of Monza, the texture of which shows an intermediate pattern between the last two, with the presence of bricks and stones, are overlapped to those of the inner leaf and those of the belfry.

A total of 4 prisms coming from the conglomerate forming the very thick internal part of the 2800 mm three-leaf medieval masonry (labeled Q, B, M and S) and 4 coming from the XVI century plain masonry (labeled Ec, W, K and In) of dimensions 200 x 200 x 350 mm were tested applying subsequent load steps of 0.3 MPa kept constant for intervals of 28800 sec. (Table 2) (Figure 8). On average, higher peak stresses (σ_f) and lower strains at failure (ε_v^{\max} , ε_h^{\max}) were registered on the XVI century plain masonry, which reached failure in a longer time than the prisms of the medieval masonry [14]. In Figure 8 the results of a test carried out on the masonry of the inner leaf and those of a test carried out on the masonry of the XVI century plain masonry are respectively shown. In particular, in the case of the XVI century masonry a more brittle behaviour can be observed, governed by the presence of the bricks that in this masonry are more regularly and abundantly present than the mortar. It is interesting to compare the trends of horizontal strain, which are differently influenced by the first crack, however showing a strong dilation in both cases. In the case of the medieval inner leaf, the observed behaviour is non-brittle, the diagram is markedly non-linear and failure is gradually reached (Figure 9a). In the case of the XVI century masonry, the diagram becomes bilinear with a change in its slope at a stress value of 3 N/mm² (Figure 9b).

This behaviour is coherent with the crack pattern at failure: in the case of the inner leaf (Figure 10a) the cracks do not cut the bricks and the stones, but mainly involve mortar and tend to propagate at the interface between mortar and resistant elements. In the case of the XVI century

masonry (Figure 10b) cracks are clearly vertical and involve both bricks and the mortar.

Considering the last load step for each specimen, the secondary creep rate before collapse has been calculated and then related to the duration of the last load step, which can be regarded as the residual life of the material. In Figure 11 these values have been plotted comparing the masonry of Monza [23], [14], [24] previously tested with those of the Tower of Pavia. An interesting inverse relationship can be found, which seems to apply to the different materials considered together, as well as to other brittle materials like concrete, subjected to creep and fatigue tests [25]. The observed strong correlation could be used as a reliable parameter to predict the residual life of a material element subjected to a given sustained stress.

THE STRAIN-RATE BEHAVIOUR APPROACHED THROUGH A PROBABILISTIC MODEL

By experimental evidence, the strain evolution connected with a given stress history of a viscous material like a historic masonry can be described through the vertical and horizontal strain-rate reached at a certain vertical stress level σ_v . Therefore, in the preservation of historic buildings from major damage or even failure it would be very useful to indicate a critical value of the strain-rate under which the residual life of the building is greater than the required service life.

As reported in Figure 11, an inverse relationship between the secondary creep strain-rate and the residual life of the material.

With the aim to investigate the residual life of material as a function of the strain-rate, the parameters $\dot{\varepsilon}_v$ and $\dot{\varepsilon}_h$ respectively defined as the vertical and horizontal strain-rate, are quantified by the slope of the linear branches of the strain versus time diagrams obtained in the experimental tests (Figure 8); their values are recorded at the constant applied stress level σ_v^* ; here and in the follow the experimental stress values will be denoted with *.

For each σ_v^* the high randomness connected with the changing of strain-rate, due to the high

non-homogeneity of the masonry, allows for the treatment of $\dot{\varepsilon}_v$ and $\dot{\varepsilon}_h$ as *random variables* (r.v.) with a certain distribution of values (Figure 12 a and b). Seen in this way, the deformation process can be interpreted as a stochastic process of the considered r.v.. The strain-rate also depends on the stress level σ_v^* , corresponding to which the deformation is recorded. Therefore, for each stress level σ_v^* , the strain-rate (measured in ε/sec) can be modelled with a probability density function (p.d.f.) $f_{\dot{\varepsilon}}(\dot{E})$, which is dependent on σ_v^* and on the strain rate. In order to model $f_{\dot{\varepsilon}}(\dot{E})$ at every stress level σ_v^* (Figure 13a and b), a family of theoretical distributions must be chosen.

Choosing the suitable p.d.f. modelling a given phenomenon is a delicate and important matter; it must be found according to the physical aspects of the phenomenon itself, and to the characteristics of the distribution function in its “tail”, where often no experimental data can be collected. This latter aspect can be investigated analyzing the behaviour of the failure rate function $\phi_{\dot{\varepsilon}}(\dot{E})$ at every stress level σ_v^* connected with the chosen distribution function:

$$\phi_{\dot{\varepsilon}}(\dot{E})d\dot{E} = \Pr\{\dot{E} < \dot{\varepsilon} \leq \dot{E} + d\dot{E} \mid \dot{\varepsilon} > \dot{E}\} \quad \forall \sigma_v^*, \quad \dot{\varepsilon} = \dot{\varepsilon}_h \quad \text{or} \quad \dot{\varepsilon} = \dot{\varepsilon}_v \quad (1)$$

The function (1) is able to describe the immediate occurrence rate of a given event. It can present three fundamental behaviours. A *constant* hazard-rate means: since that a system has functioned for some time without failing, there is no effect on the failure probability for the period ahead. A *decreasing* failure rate means that the failure probability for the period ahead is favourably affected by the system satisfactory functioning for a certain time. An *increasing* failure rate means that the system has already been in service for some time and has reduced its reliability, so that its probability of failure is increasing. In an actual material, a combination of these respective cases is possible. More details on this subject are given in [26] and [27].

Considering the recorded experimental data, a conventional value of $\dot{\varepsilon}$ may be assumed as a critical value indicating a safety limit. Consequently, for a given stress level σ_v^* the probability to record the critical strain-rate connected with the secondary creep safety limit increases if the strain-

rate increases. In other words, at a given stress level σ_v^* , the probability that the secondary creep strain-rate falls in the interval $\{\dot{E} < \dot{\epsilon} \leq \dot{E} + d\dot{E}\}$ increases as the strain-rate increases. This hypothesis, assumed as a satisfying (but not unique) physical interpretation of the decay process, associated with the information given by (1) on the hazard rate behaviour of various p.d.f. families, leads to model the behaviour of the strain-rate at the stress level σ_v^* with a Weibull p.d.f. as follows:

$$f_{\dot{\epsilon}}(\dot{E}) = \alpha_1 \rho_1 (\rho_1 \dot{E})^{\alpha_1 - 1} \exp\left[-(\rho_1 \dot{E})^{\alpha_1}\right] \quad \forall \sigma_v^* \quad (2)$$

This family of distributions presents an hazard rate function (1) which increases if the value of \dot{E} increases and tends to ∞ if $\dot{E} \rightarrow \infty$; this fact seems to respect the physical interpretation of the strain-rate behaviour previously proposed.

The strain-rate behaviour as a reliability problem

It is furthermore interesting to evaluate the probability that the system will reach, or exceed a given strain-rate level $\bar{\epsilon}_h$ or $\bar{\epsilon}_v$ over a stress history. Considering a significant strain-rate level $\bar{\epsilon}_h$ or $\bar{\epsilon}_v$ and the variable stress needed to exceed it, the strain-rate behaviour can be treated as a reliability problem, [27], [28].

Reliability $R(t)$ is related to the performance of a system over time, and is defined as the probability that the system does not fail by time t . This definition is extended here, denoting by $\bar{R}(\sigma_v)$ the probability that a system will not exceed a given significant strain-rate level by stress σ_v . The random variable that is used to quantify reliability is $\bar{\sigma}$, which is simply the stress it takes to exceed damage $\bar{\epsilon}_h$ or $\bar{\epsilon}_v$. Thus, from this point of view, the reliability function is given by [29]:

$$\bar{R}(\sigma_v) = \Pr(\bar{\sigma} > \sigma_v) = 1 - F_{\bar{\sigma}}(\sigma_v) \quad (3)$$

where $F_{\bar{\sigma}}(\sigma_v)$ is the distribution function for $\bar{\sigma}$.

Computing $F_{\bar{\sigma}}(\sigma_v)$ for different damage levels $\bar{\epsilon}_h$ (or $\bar{\epsilon}_v$) allows us to build the corresponding

fragility curves describing the probability of exceeding a given strain-rate over stress [30] that is expressed as the area above the threshold $\bar{\dot{\epsilon}}_h$ (or $\bar{\dot{\epsilon}}_v$) (Figure 14) and can be calculated by using the survive function:

$$\mathfrak{S}_{\dot{\epsilon}}(\dot{E}) = 1 - F_{\dot{\epsilon}}(\dot{E}) \quad \forall \quad \sigma_v^* \quad (4)$$

where $F_{\dot{\epsilon}}(\dot{E})$ is the cumulative distribution function of the p.d.f. (2) at every σ_v^* . The computation of $\mathfrak{S}_{\dot{\epsilon}}(\dot{E})$ at every σ_v^* is possible with the use of any kind of computer code for numerical integration. The areas computed over different strain rate thresholds provide the experimental fragility curves $F_{\sigma^*}(\sigma_v)$. In other words, the probability to exceed a certain level $\bar{\dot{\epsilon}}_h$ (or $\bar{\dot{\epsilon}}_v$) at different experimental stress values σ_v^* can be plotted in graphical form here called *experimental fragility curve*: for each $\bar{\dot{\epsilon}}_h$ (or $\bar{\dot{\epsilon}}_v$) chosen an experimental fragility curve can be built.

Since the experimental fragility curves are composed by a discrete number of points (Figure 15) to describe their behaviour over σ_v a probabilistic modelling is needed. To make it we must assume that the density function $f_{\bar{\sigma}}(\sigma_v)$ exists for the r.v. $\bar{\sigma}$, the failure rate function $\phi_{\bar{\sigma}}(\sigma_v)$ is given by [29]:

$$\phi_{\bar{\sigma}}(\sigma_v) = \frac{f_{\bar{\sigma}}(\sigma_v)}{\bar{R}(\sigma_v)} \quad (5)$$

To model the experimental fragility curves, a Weibull distribution has been chosen [21, 27, 31, 33] that seems to provide a good interpretation of the physical phenomenon. In fact, experimental evidence indicates that the failure rate function $\phi_{\bar{\sigma}}(\sigma_v)$ has a polynomial form and, consequently, must be [29, 31]:

$$\phi_{\bar{\sigma}}(\sigma_v) = b_1 \sigma_v^{b_2} \quad (6)$$

where $b_1 > 0$ and $-1 < b_2 < +\infty$ are constants.

Since $\bar{R}(\sigma_v) = \exp\left\{-\int_0^{\sigma_v} \phi_{\bar{\sigma}}(u) du\right\}$ and $f_{\bar{\sigma}}(\sigma_v) = \phi_{\bar{\sigma}}(\sigma_v) \exp\left\{-\int_0^{\sigma_v} \phi_{\bar{\sigma}}(u) du\right\}$ and assuming: $b_1 = \alpha \rho^\alpha$ and $b_2 + 1 = \alpha$ (with α and ρ equal constants) we obtain:

$$\int_0^{\sigma_v} \phi_{\sigma}(u) du = \frac{b_1 \sigma_v^{b_2+1}}{b_2+1} = (\rho \sigma_v)^{\alpha} \quad (7)$$

$$\text{Therefore: } \bar{R}(\sigma_v) = \exp[-(\rho \sigma_v)^{\alpha}] \quad (8)$$

which is definitely the well known Weibull survive function [29], [32].

As a consequence of this, for different strain-rate levels $\bar{\dot{\epsilon}}_h$, the distribution $F_{\sigma}(\sigma_v)$ involved in (3), through (8), will be a Weibull distribution [29]; it allows for computing the theoretical fragility curves through which the “failures” with a higher or lower probability of occurrence at the given stress σ_v can be identified. The shape parameters involved in the distributions used have been estimated through a computer code using the least squares and the Rosenbrock’s optimization methods.

INTERPRETATION OF THE PSEUDO-CREEP TESTS

The described procedure has been applied here to the life-time estimate of ancient masonry, modelling the results obtained from the pseudo-creep tests mentioned above. Some results of this research were presented in [34], [35]; here new elaborations on masonry of different ages and different textures are introduced to support the previous results obtained and to investigate the potentiality of the model to model different kind of masonry.

An important step is the identification of significant thresholds of critical strain. This choice can be made considering the slope of the strain vs. time diagram in the branch corresponding to the secondary creep phase during the last load step (Figure 6). The tangent to this branch represents the strain rate limit value corresponding to which the material reaches failure. Therefore, the strain rate chosen as safety threshold should certainly be lower than such value. In this case, the assumed critical strain rates are: $\bar{\dot{\epsilon}}_v = 5.0 \times 10^{-5}$ and $\bar{\dot{\epsilon}}_v = 1.0 \times 10^{-4}$; the same values have been assumed also for $\bar{\dot{\epsilon}}_h$.

Here in the following the proposed probabilistic approach is used to investigate the probability of

failure of the medieval inner leaf masonry and of the XVI century plain masonry of the Civic Tower of Pavia (Figure 2) due to its permanent load using experimental data. The procedure has been applied to evaluate the influence of the vertical and horizontal deformation on the collapse of the structure.

The medieval inner leaf masonry

Figure 15 shows the fragility curves describing the behaviour of the medieval inner leaf masonry. It appears that, in the case of $\bar{\varepsilon}_h = \bar{\varepsilon}_v = 5.0 \times 10^{-5}$, the same probability level corresponds to a higher stress value σ_v for the horizontal strain than for the vertical one. In other words, if the vertical strain is considered, the critical threshold 5.0×10^{-5} is reached at a relatively low stress value. In fact, at low strain level, the masonry behaviour keeps within the elastic limit, consequently the direct strain (parallel to the load direction) are prevailing. This phenomenon inverts if a higher threshold is considered ($\bar{\varepsilon}_h = \bar{\varepsilon}_v = 1.0 \times 10^{-4}$).

In this case, at the same probability level, vertical strain corresponds to a higher value of σ_v than that shown by the horizontal strain; this means that in the case of horizontal strain the critical threshold 1.0×10^{-4} is reached at lower values than those shown by the vertical strain (Table 3).

This depends on the mechanical damage developed during the test due to the load increase: in fact, the exit from the elastic range implies the preponderance of the horizontal (indirect) strain on the vertical ones which can be denominated dilation. In the case of the threshold 1.25×10^{-5} , the horizontal and vertical fragility curves apparently are exactly the same (Figure 16). Really, given the low distribution of the experimental data, all situated close to the value 1, the modelling is not much indicative of the real material behaviour: it is rather a symptom of it and, in this case, the prediction has to be assumed with caution.

The XVI century plain masonry

Figures 17 and 18 show the fragility curves relative to the XVI century plain masonry for three critical thresholds: 5.0×10^{-5} and 1.0×10^{-4} (Figure 17); 1.25×10^{-5} (Figure 18). In Figure 17b, the fragility curve describing the probability of exceeding the vertical critical threshold $\bar{\varepsilon}_v$ is modelled through a Weibull distribution, like in the case of the inner leaf. In this case the experimental data are more scattered around the theoretical curves.

A difference has to be highlighted in the case of the horizontal strain. The experimental values show a bimodal behaviour (Figure 17a); therefore, in this case a mixture of two distributions had to be adopted for the modelling:

$$F_{\bar{\sigma}}(\sigma) = p \cdot w_1 + (1 - p) \cdot w_2 \quad (9)$$

where w_1 and w_2 are two Weibull distributions with different shape parameters, respectively modelling the behaviour *before* the threshold $\sigma_v = 2N/mm^2$ and *after* such threshold (Figure 17a). Parameter p represents the percentage value of experimental probability influencing the first distribution, whereas $(1 - p)$ is its reciprocal.

The discontinuity on the fragility curves corresponds to the neat change in the slope of the diagram relative to the horizontal strain (Figure 9b) associated to the brittle behaviour of the XVI century masonry. Such brittleness depends on the failure mechanism governed by the brick cracking, as already underlined by the analysis of the crack patterns (Figure 10b).

In Figure 18 for the case of the threshold 1.25×10^{-5} the horizontal and vertical fragility curves are plotted. In Figure 18a the bi-modal behaviour is evident however, given the low distribution of the experimental data, both in Figure 18a and in Figure 18b the points of the experimental fragility curves are all situated close to the value 1 as in Figure 16. Therefore, also this time, the modelling is not much indicative of the real material behaviour: it is rather a symptom of it and, in this case, the prediction has to be assumed with caution.

In Table 4 a dilatant behaviour of the XVI century plain masonry is highlighted by the stress values corresponding to the exceedance of all the three critical thresholds 1.25×10^{-5} , 5.0×10^{-5} and

1.0×10^{-4} , always lower in the case of the horizontal strain than the vertical. For all the considered thresholds, the behaviour of the material can be considered external to the elastic range, since the indirect strains are always prevailing on the vertical ones.

CONCLUSIONS

The time-dependent behaviour, together with other factors acting in a synergetic way, proved to be responsible of the collapse of some monumental buildings happened during the last fifteen years. The problem has been faced through an experimental programme showing that laboratory pseudo-creep tests provide useful results for a deeper knowledge of the primary, secondary and tertiary creep phases. The applied probabilistic model seems to appropriately interpret the experimental results, allows an estimate of the exceedance of the critical thresholds in vertical and horizontal strain rate that are related to the residual service life, and also captures the difference between masonry of different ages and characteristics.

For the safety assessment of time-dependent historic masonry buildings, useful information aimed to the prevision of the residual life may be provided by in-situ long-term monitoring campaigns recording the evolution of the main crack opening and/or the variations of masonry wall thickness combined with complementary information on the states of stress and on the quality of masonry recorded through single and double flat-jack tests and sonic tests. The results obtained through the proposed probabilistic approach indicate an interesting research direction toward the interpretation of data collected through the monitoring of monumental buildings, to prevent total or partial failure. The precocious recognition in-situ of critical values of secondary creep strain rate related to the residual service life will allow to design strengthening interventions finalized both to directly repair damage and to remove the vulnerability sources.

ACKNOWLEDGEMENTS

Ms Serena Sironi and Ms Roberta Tassi are gratefully acknowledged for their assistance in the experimental work and data elaboration; Mr Marco Antico for his technical support in the

laboratory. The research has been supported by COFIN 2002 MIUR funds.

REFERENCES

- [1] Goodman, R. E. Rock Mechanics. John Wiley & Sons, Inc., New York, 1989.
- [2] Jaeger JC, Cook NG. Fundamentals of rock mechanics. 2nd edition, Chapman & Hall, London, 1976.
- [3] Enright MP, Frangopol DM. Failure Time Prediction of Deteriorating Fail-Safe Structures. Journal of Structural Engineering, ASCE, USA, 124(12), 1448-1457, 1998.
- [4] Sarja A, Vesikari E. Durability Design of Concrete Structures. RILEM Report 14, RILEM Technical Committee 130-CSL, E & FN Spon, 1996.
- [5] Biondini F, Bontempi F, Frangopol DM, Malerba PG. Cellular Automata Approach to Durability Analysis of Concrete Structures. Journal of Structural Engineering, ASCE, USA, 130(11), 1724-1737, 2004.
- [6] Biondini F, Bontempi F, Frangopol DM, Malerba PG. Probabilistic Service Life Assessment and Maintenance Planning of Concrete Structures. Journal of Structural Engineering, ASCE, USA, 132(5), 810-825, 2006.
- [7] Mori Y, Ellingwood B. Reliability-based service-life assessment of aging concrete structures. Journal of Structural Engineering ASCE, 119(5), 159-176, 1993.
- [8] Val DV, Melchers R. E. Reliability of deteriorating RC slab bridges. Journal of Structural Engineering ASCE, 123(12), 1638-1644, 1997.
- [9] Ibarra L, Krawinkler H. Effect of uncertainty in system deterioration parameters on the variance of collapse capability. ICOSSAR'05, Int. Conf. on Structural Safety and Reliability; Rome, Italy, 2005, G. Augusti, G.I. Schuëller, M. Ciampoli Eds. Millpress, Rotterdam, The Nethetland, CD-ROM, 3583-3590, 2005.
- [10] Bentz DP, Garboczi EJ. Modelling the Leaching of Calcium Hydroxide from Cement Paste: Effects of Pore Space Percolation and Diffusivity. Materials and Structures, 25, 523-533, 1992.
- [11] Papa E, Taliercio A, Binda L. Creep Failure of Ancient Masonry: Experimental

Investigation and Numerical Modeling, 7th SSRMHB, Int. Conf. Structural Studies, Repairs, and Maintenance of Historic Buildings; Bologna, Italy, 2001, Ed. C.A. Brebbia, 285-294, 2001.

[12] Papa E, Taliercio A. A theoretical model for the description of static and creep-induced damage in brittle materials under non-proportional loading. Computational Plasticity VII – Fundamentals and Applications; Barcelona, Spain, 2003, eds. Owen D.R.J., Oñate E., Suárez B., CIMNE, CD ROM, 2003.

[13] Anzani A, Binda L, Taliercio A. Experimental and numerical study of the long term behaviour of ancient masonry. 9th STREMAH, Int. Conf. on Structural Studies, Repairs and Maintenance of Heritage Architecture; Eds. C.A. Brebbia, A. Torpiano, Malta, 2005, Section 9, 577-586, 2005.

[14] Anzani A, Binda L, Taliercio A. Application of a damage model to the study of the long term behavior of ancient towers. 1st Canadian Conference on Effectiveness Design of Structures; Hamilton, Ontario, Canada, 2005, CD-ROM, 401-412, 2005.

[15] Valluzzi MR, Modena C. Mechanical behaviour of masonry structures strengthened with different improvement techniques. Fracture and Failure of Natural Building Stones, Springer Netherlands, 137-156, 2006.

[16] Casolo S. Modelling in-plane micro-structure of masonry walls by rigid elements. International Journal of Solids and Structures, Elsevier Science Ltd, 41(13), 3625-3641, 2004.

[17] Anzani A, Binda L, Melchiorri G. Time dependent damage of rubble masonry walls. Proceedings of the British Masonry Society London, UK, 7(2), 341-351, 1995.

[18] Binda L, Anzani A. The time-dependent behaviour of masonry prisms: an interpretation. The Masonry Society Journal, 2(11), 17-34, 1993.

[19] Anzani A, Binda L, Mirabella Roberti, G. The effect of heavy persistent actions into the behaviour of ancient masonry. Materials and Structures, 33, May, 251-261, 2000.

[20] Anzani A, Binda L, Mirabella Roberti G. Experimental researches into long term behaviour of historical masonry. L. Binda (ed. by) Learning from failure, WIT Press, Southampton, UK,

Chapt. 2, 2007.

- [21] Bekker PCF. Durability Testing of Masonry: Statistical Models and Methods. *Masonry International*, 13(1), 32-38, 1999.
- [22] Binda L, Gatti G, Mangano G, Poggi C, Sacchi Landriani G. The collapse of the Civic Tower of Pavia: a survey of the materials and structure. *Masonry International*, 6(1), 11-20, 1992.
- [23] Anzani A, Binda L, Garavaglia E. Simple checks to prevent the collapse of heavy historical structures and residual life prevision through a probabilistic model. L. Binda (ed. by), *Learning from failure*, WIT Press, Southampton, UK, Chapt. 9, 205-223, 2007.
- [24] Mirabella Roberti G, Binda L, Anzani A., Experimental investigation into the effects of persistent and cyclic loads on the masonry of ancient towers. 7th Int. Conf. on Structural Faults and Repair; M. C. Forde Ed., Engineering Technics Press, Edinburgh, 3, 339-347, 1997.
- [25] Taliercio A, Gobbi E. Fatigue Life and Change in Mechanical Properties of Plain Concrete Under Triaxial Deviatoric Cyclic Stresses. *Magazine of Concrete Research*, 50(3), pp. 247-256, 1998.
- [26] Binda L, Molina C. Building Materials Durability Semi-Markov Approach. *Journal of Materials in Civil Engineering*, ASCE, USA, 2(4), 223–239, 1990.
- [27] Garavaglia E, Gianni A, Molina C. Reliability of Porous Materials: Two Stochastic Approaches. *Journal of Materials in Civil Engineering*, ASCE, USA, 16(5), 419-426, 2004.
- [28] Garavaglia E, Anzani A, Binda L. Application of a Probabilistic Model to the Assessment of Historic Building Under Permanent Loading. 4th Int. Seminar “Structural Analysis of Historical Constructions”; Padua, 2004, 1, pp. 589-596, 2004.
- [29] Evans DH. *Probability and its Applications for Engineers*, Marcel Dekker, Inc., New York, NJ, USA, 1992.
- [30] Singhal A, Kerimidjian AS. Method for Probabilistic Evaluation of Seismic Structural Damage. *Journal of Structural Engineering*, ASCE, 122(12), 1459-1467, 1996.
- [31] Garavaglia E, Lubelli B, Binda L. Two Different Stochastic Approaches Modelling the

Deterioration Process of Masonry Wall over Time. *Materials and Structures*, 248(35), 246-256, 2002.

[32] Cox DR. *Renewal Theory*. Methuen LTD, London, UK, EU.1962

[33] Cranmer DC, Richerson, D.W. *Mechanical Testing Methodology for Ceramic Design and Reliability*. Marcel Dekker Inc., New York, NJ, USA, 1998.

[34] Anzani A, Garavaglia E, Binda L. A Probabilistic Approach for the Interpretation of Long Term Damage of Historic Masonry. 10th Canadian Masonry Symposium; Banff, Alberta, Canada, 2005, Ed. S. Lissen, C. Benz, M. Hagel, C. Yuen, N. Shrive, Printed by Dept. of Civil Eng. The University of Calgary, Canada, I, 664-673, 2005.

[35] Garavaglia E, Anzani A, Binda L. A Probabilistic Model for the Assessment of Historic Buildings under Permanent Loading. *Journal of Materials in Civil Engineering*, ASCE, 18(6), 858-867, 2006.

FIGURE CAPTIONS

Figure 1. Primary, secondary and tertiary creep phases at constant uniaxial compression stress.

Figure 2. Civic Tower of Pavia: (a) before failure, (b) detail of the 2800 mm thick medieval masonry.

Figure 3. Results of a cyclic test on a 400 x 600 x 700 mm masonry prism.

Figure 4. Prisms of 300 x 300 x 510 mm from the inner leaf: results of creep tests.

Figure 5. Pseudo-creep tests on a 100 x 100 x 180 mm prism of the inner leaf.

Figure 6. Characterization of the specimens by (a) sonic tests and (b) monotonic tests: (---) inner leaf, (—) XVI century plain masonry. Figure 1. Pavia, outer leaf.

Figure 7. Masonry specimens belonging to a) Pavia, outer leaf, b) Pavia, inner leaf, c) Pavia, belfry, d) Monza, Crypt.

Figure 8. Pseudo-creep curves: (---) inner leaf, (—) XVI century plain masonry; letters

indicate individual specimens quoted in tab. 2.

Figure 9. Pseudo creep tests: (a) on prism In of the inner leaf, (b) on prism M, XVI century masonry.

Figure 10. Crack pattern at the end of pseudo creep tests: (a) on prism In of the inner leaf, (b) on prism M of the XVI century masonry.

Figure 11. Secondary creep strain rate vs. duration of last load step.

Figure 12. Interpolation of the vertical (a) and horizontal (b) strain-rate vs. applied stress.

Figure 13. Vertical (a) and horizontal (b) secondary creep strain-rate vs. applied stress (***) modelled with a Weibull p.d.f $f_{\dot{\epsilon}}(\dot{E})$ (—).

Figure 14. Exceedance probability to cross the threshold $\bar{\dot{\epsilon}}$

Figure 15. Inner leaf medieval masonry: experimental ($\blacktriangle \bar{\dot{\epsilon}}_h, \bar{\dot{\epsilon}}_v = 5.0 \times 10^{-5}$, $\bullet \bar{\dot{\epsilon}}_h, \bar{\dot{\epsilon}}_v = 1.0 \times 10^{-4}$) and theoretical (—) fragility curves; a) horizontal strain-rate, b) vertical strain-rate.

Figure 16. Inner leaf medieval masonry: experimental (\bullet) and theoretical (—) fragility curves; a) horizontal strain-rate, b) vertical strain-rate. Critical strain-rate threshold: 1.25×10^{-5} .

Figure 17. XVI century plain masonry: experimental ($\blacktriangle \bar{\dot{\epsilon}}_h, \bar{\dot{\epsilon}}_v = 5.0 \times 10^{-5}$, $\bullet \bar{\dot{\epsilon}}_h, \bar{\dot{\epsilon}}_v = 1.0 \times 10^{-4}$) and theoretical (—) fragility curves; a) horizontal strain-rate, b) vertical strain-rate.

Figure 18. XVI century plain masonry: experimental (\bullet) and theoretical (—) fragility curves; a) horizontal strain-rate, b) vertical strain-rate. Critical strain-rate threshold: 1.25×10^{-5} .

TABLE CAPTIONS

Table 1. Average results of pseudo creep tests on specimens of dimension 100x100x180 mm

Table 2. Results of pseudo creep tests of the second series.

Table 3. Medieval inner leaf: Probability to exceed $\bar{\varepsilon}_h$ and $\bar{\varepsilon}_v$ for different σ_v , $\bar{\varepsilon}_h$ and $\bar{\varepsilon}_v$.

Table 4. XVI century plain masonry: Probability to exceed $\bar{\varepsilon}_h$ and $\bar{\varepsilon}_v$ for different σ_v , $\bar{\varepsilon}_h$ and

$\bar{\varepsilon}_v$.

TABLES

Table 1.

Average results of pseudo creep tests on specimens of dimension 100x100x180 mm.

Time interval [sec]	σ_F [MPa]	ε_v^{\max} ($\times 10^3$)
300	3.68	3.17
900	2.73	4.20
3600	2.47	4.12
10800	2.68	5.87

Table 2.

Results of pseudo creep tests of the second series.

specimen	masonry	σ_f [MPa]	ε_v^{\max} [$\mu\text{m}/\text{mm}$]	ε_h^{\max} [$\mu\text{m}/\text{mm}$]
prism Q	belfry	6,07	9,52	-20,39
prism B		4,36	5,98	-26,46
prism M		5,27	4,67	-15,56
prism S		4,13	7,19	-17,23
<i>average</i>		4,96	6,84	-19,91
prism Ec	inner leaf	3,59	8,43	-11,84
prism W		2,75	4,00	-7,89
prism K		1,56	3,99	-45,35
prism In		2,47	4,78	-18,30
<i>average</i>		2,59	5,30	-20,85

Table 3.

Medieval inner leaf: Probability to exceed $\bar{\varepsilon}_h$ and $\bar{\varepsilon}_v$ for different σ_v , $\bar{\varepsilon}_h$ and $\bar{\varepsilon}_v$.

	$\bar{\varepsilon}_h = 0.0000125$	$\bar{\varepsilon}_v = 0.0000125$	$\bar{\varepsilon}_h = 0.00005$	$\bar{\varepsilon}_v = 0.00005$	$\bar{\varepsilon}_h = 0.0001$	$\bar{\varepsilon}_v = 0.0001$
Ex. pr. of $\bar{\varepsilon}_v$	σ_v (N/mm ²)	σ_v (N/mm ²)	σ_v (N/mm ²)	σ_v (N/mm ²)	σ_v (N/mm ²)	σ_v (N/mm ²)
10%	0.682	0.631	0.139	0.002	0.147	0.158
63%	0.825	0.832	0.648	0.054	0.791	1.382
90%	0.899	0.901	1.153	0.849	1.476	2.022

Table 4.

XVI century plain masonry: Probability to exceed $\bar{\varepsilon}_h$ and $\bar{\varepsilon}_v$ for different σ_v , $\bar{\varepsilon}_h$ and $\bar{\varepsilon}_v$.

	$\bar{\varepsilon}_h = 0.0000125$	$\bar{\varepsilon}_v = 0.0000125$	$\bar{\varepsilon}_h = 0.00005$	$\bar{\varepsilon}_v = 0.00005$	$\bar{\varepsilon}_h = 0.0001$	$\bar{\varepsilon}_v = 0.0001$
Ex. pr. of $\bar{\varepsilon}_v$	σ_v (N/mm ²)	σ_v (N/mm ²)	σ_v (N/mm ²)	σ_v (N/mm ²)	σ_v (N/mm ²)	σ_v (N/mm ²)
10%	0.005	0.150	0.150	0.700	0.897	1.100
63%	0.350	0.875	1.375	1.833	2.267	2.781
90%	1.320	1.650	2.450	2.652	2.675	3.924

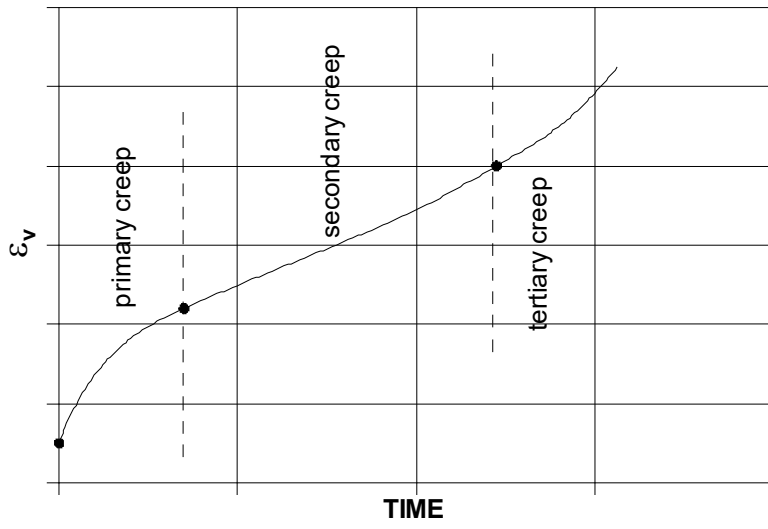


Figure 1. Primary, secondary and tertiary creep phases at constant uniaxial compression stress.



Figure2. Civic Tower of Pavia: (a) before failure, (b) detail of the 2800 mm thick medieval masonry.

colour version

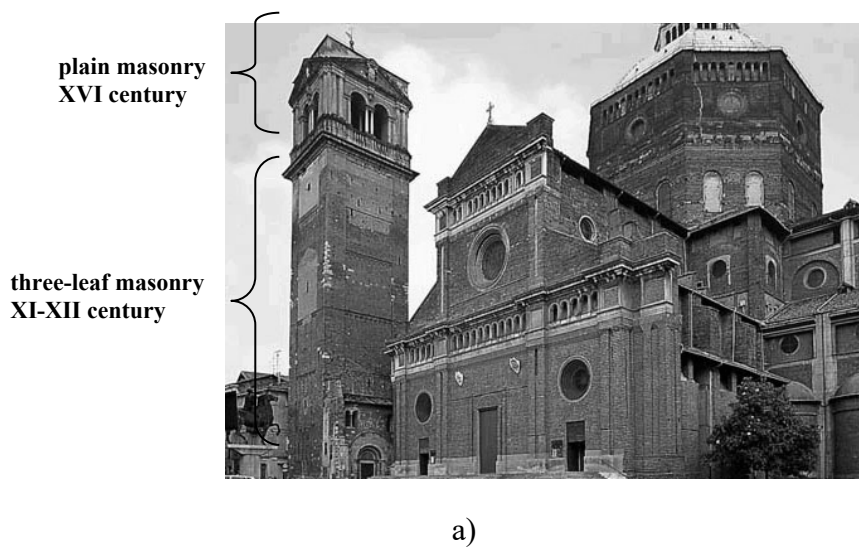


Figure 2. Civic Tower of Pavia: (a) before failure,
(b) detail of the 2800 mm thick medieval masonry.

black and white version

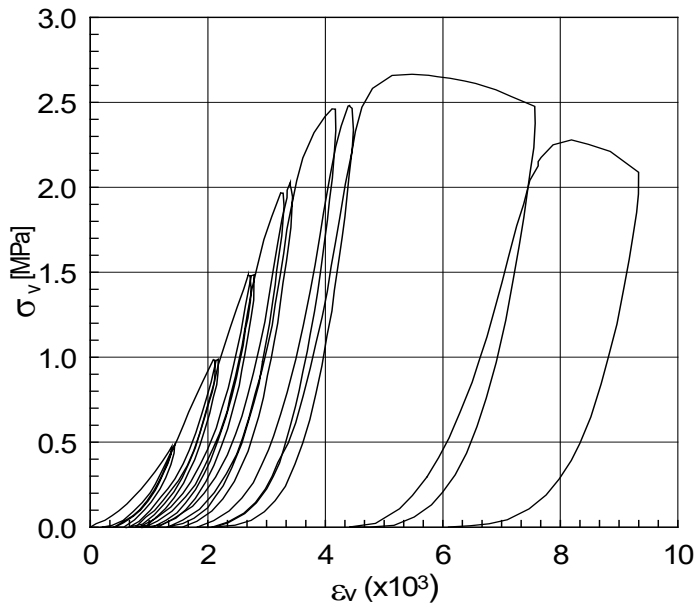
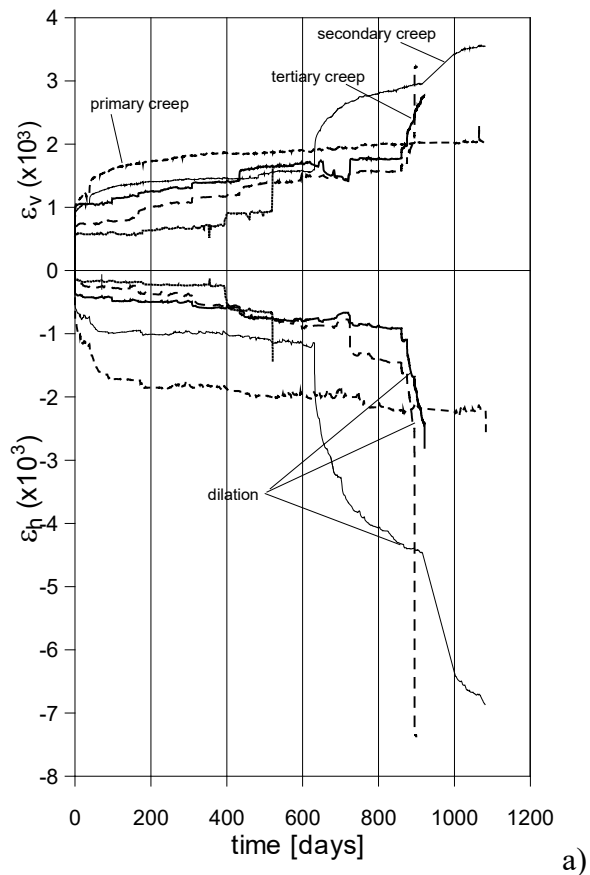
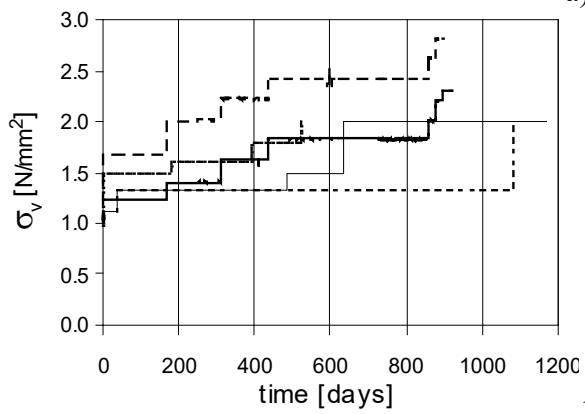


Figure 3. Results of a cyclic test on a 400 x 600 x 700 mm masonry prism.



a)



b)

Figure 4. Prisms of 300 x 300 x 510 mm from the inner leaf: results of creep tests.

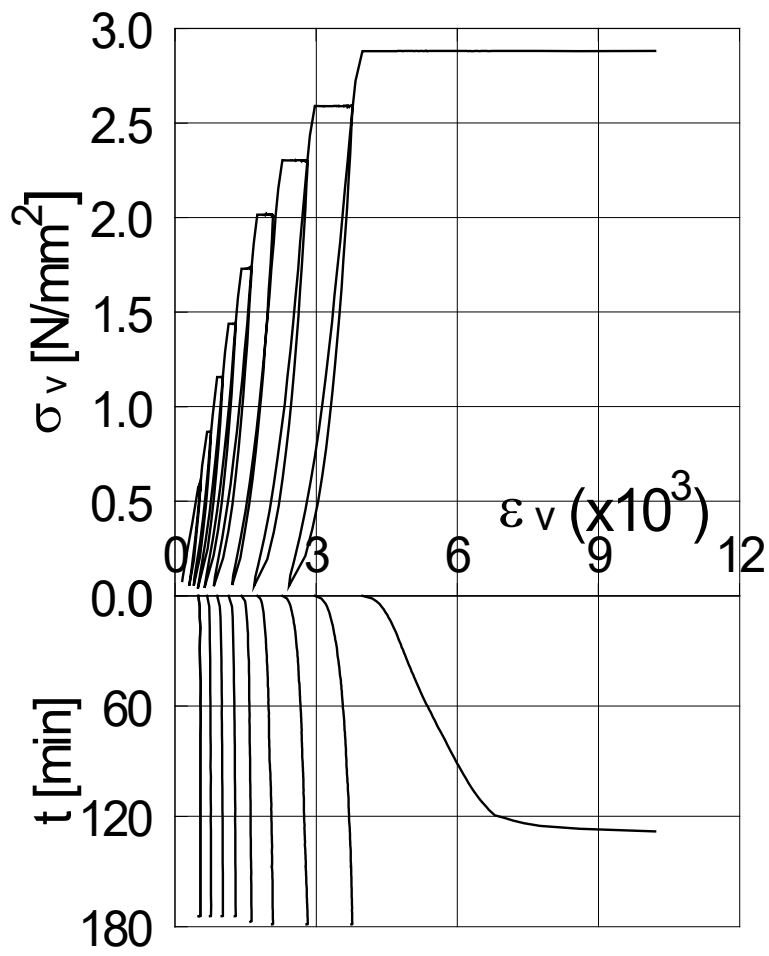


Figure 5. Pseudo-creep tests on a 100 x 100 x 180 mm prism of the inner leaf.